A Ternary Metal Binding Site in the C2 Domain of Phosphoinositide-Specific Phospholipase C-δ1[†,‡]

Lars-Oliver Essen,[§,‖] Olga Perisic,[§] Denise E. Lynch,[§] Matilda Katan,[⊥] and Roger L. Williams*,[§]

Centre for Protein Engineering, MRC Centre, Hills Road, Cambridge CB2 2QH, U.K., and CRC Centre for Cell and Molecular Biology, Chester Beatty Laboratories, Fulham Road, London SW3 6JB, U.K.

ABSTRACT: We have determined the crystal structures of complexes of phosphoinositide-specific phospholipase C-δ1 from rat with calcium, barium, and lanthanum at 2.5−2.6 Å resolution. Binding of these metal ions is observed in the active site of the catalytic TIM barrel and in the calcium binding region (CBR) of the C2 domain. The C2 domain of PLC-δ1 is a circularly permuted topological variant (P-variant) of the synaptotagmin I C2A domain (S-variant). On the basis of sequence analysis, we propose that both the S-variant and P-variant topologies are present among other C2 domains. Multiple adjacent binding sites in the C2 domain were observed for calcium and the other metal/enzyme complexes. The maximum number of binding sites observed was for the calcium analogue lanthanum. This complex shows an array-like binding of three lanthanum ions (sites I−III) in a crevice on one end of the C2 β-sandwich. Residues involved in metal binding are contained in three loops, CBR1, CBR2, and CBR3. Sites I and II are maintained in the calcium and barium complexes, whereas sites II and III coincide with a binary calcium binding site in the C2A domain of synaptotagmin I. Several conformers for CBR1 are observed. The conformation of CBR1 does not appear to be strictly dependent on metal binding; however, metal binding may stabilize certain conformers. No significant structural changes are observed for CBR2 or CBR3. The surface of this ternary binding site provides a cluster of freely accessible liganding positions for putative phospholipid ligands of the C2 domain. It may be that the ternary metal binding site is also a feature of calcium-dependent phospholipid binding in solution. A ternary metal binding site might be a conserved feature among C2 domains that contain the critical calcium ligands in their CBR's. The high cooperativity of calcium-mediated lipid binding by C2 domains described previously is explained by this novel type of calcium binding site.

Mammalian phosphoinositide-specific phospholipases C (PI-PLC, EC 3.1.4.11)[1] generate two second messengers, D-*myo*-inositol 1,4,5-trisphosphate (1,4,5-IP$_3$) and *sn*-1,2-diacylglycerol (DAG), by catalyzing the hydrolysis of the phospholipid phosphatidylinositol 4,5-bisphosphate (Rhee & Choi, 1992; Lee & Rhee, 1995). The second messenger 1,4,5-IP$_3$ induces the increase of intracellular calcium levels by

binding to 1,4,5-IP$_3$ receptors (Berridge, 1993), whereas diacylglycerol activates protein kinase C.

Structural work on one mammalian PI-PLC isozyme, PLC-δ1, revealed the basic domain organization of this enzyme class. PLC-δ1 (756 residues, MW 85 kDa) consists of an N-terminal membrane-anchoring PH domain (Ferguson et al., 1995a) and a catalytic core (Essen et al., 1996) that includes an EF-hand domain, the catalytic TIM-barrel domain, and, at its C-terminus, a putative membrane binding C2 domain (Figure 1). β and γ isozymes extend this architecture by adding domains responsible for specific interactions with G-protein subunits or tyrosine kinases. Besides the catalytic TIM barrel, catalytic activity strictly requires the C-terminal half of the EF-hand domain and an intact C2 domain (Ellis et al., 1993; Nakashima et al., 1995). The PH domain is not essential for catalytic activity but facilitates anchoring of PLC-δ1 on the plasma membrane (Paterson et al., 1995) and consequently enables processive catalysis (Cifuentes et al., 1993).

C2 domains appear to have several binding targets, and like other binding modules, such as SH2, SH3, or PH domains, they are common structural motifs with functional variations found in multidomain proteins involved in signal transduction and membrane trafficking. Calcium-mediated binding to anionic phospholipids is a function typical for C2 domains in calcium-regulated proteins. Some examples are protein kinase Cβ (Shao et al., 1996), cytosolic phospholipase A2 (Nalefski et al., 1994), rabphilin 3A (Yamagu-
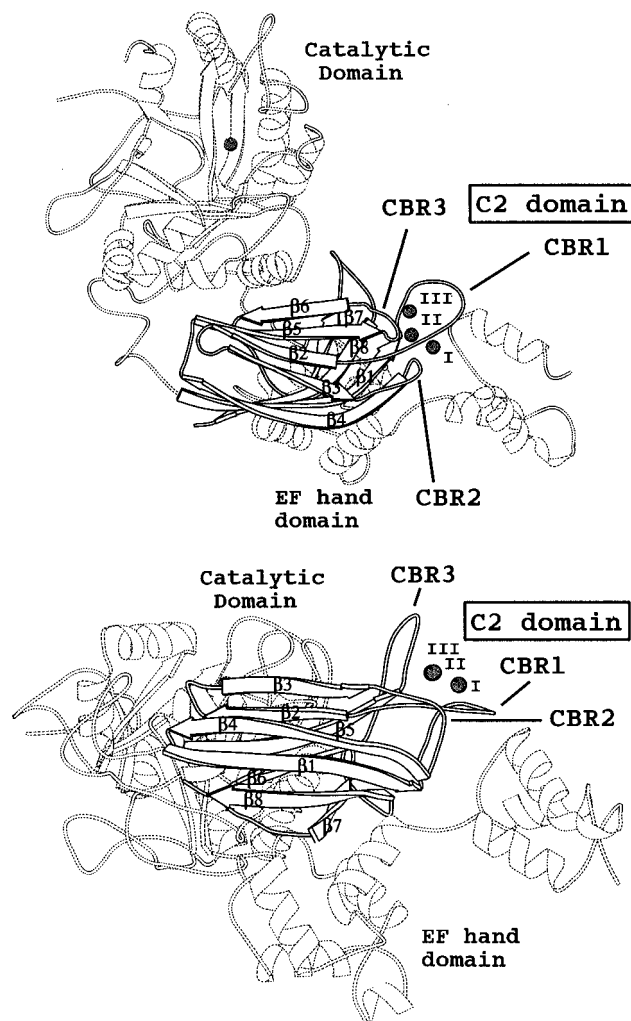
FIGURE 1: Overall structure of phospholipase C-δ1 showing the catalytic core. The C-terminal C2 domain is drawn in solid lines. Two perpendicular views are shown. Three lanthanum sites in the C2 domain and a lanthanum in the active site of the catalytic domain are represented with spheres. The diagrams were generated using MOLSCRIPT (Kraulis, 1991).

chi et al., 1993), and synaptotagmin I (Davletov & Südhof, 1993). The high cooperativity of calcium-dependent phospholipid binding—Hill coefficients between 3 and 4 are typical—suggests multiple, interacting binding sites for calcium and phospholipids on these C2 domains (Davletov & Südhof, 1993; Fukuda et al., 1996). Other calcium-dependent functions reported so far include protein binding (Li et al., 1995) and homooligomerization (Sugita et al., 1996). Some subsets of C2 domains also exhibit calcium-independent binding of phospholipids (Fukuda et al., 1994; Li et al., 1995), inositol polyphosphates (Fukuda et al., 1994; Cullen et al., 1995; (Irvine & Cullen, 1996), and proteins (Zhang et al., 1994).

Two crystal structures of C2 domains are currently known, the C2 domain in PLC-δ1 (Essen et al., 1996; Grobler et al., 1996) and the C2A domain from synaptotagmin I (SytI) (Sutton et al., 1995). The C2 domains from both proteins share an antiparallel, eight-stranded β-sandwich architecture but differ topologically by a circular permutation (Essen et al., 1996). In spite of this topological difference, the calcium binding region (CBR) of both C2 domains was found to reside on the same end of the β-sandwich. Crystallographic studies on PLC-δ1 with lanthanum as a calcium analogue

revealed that three loops of this region (CBR1, residues 643–653; CBR2, residues 675–680; CBR3, residues 706–714) are involved in binding adjacent metal ions, and two principal (highest electron density) metal binding sites were described (Essen et al., 1996). A lower resolution study on a triclinic crystal form of PLC-δ1 in a complex with the calcium analogue samarium detected the same two sites and suggested additionally that CBR1 and CBR3 undergo conformational changes during metal binding (Grobler et al., 1996). In contrast, the crystal structure of the SytI C2A domain showed only a single calcium binding site involving CBR1 and CBR3 without major structural changes. However, these crystals were sensitive to calcium concentrations greater than 100 μM. Recent NMR experiments at higher calcium concentrations supported the presence of a binary calcium binding site in the C2 domains of synaptotagmin I and protein kinase Cβ (Shao et al., 1996). Two significant differences between the reported binary calcium binding sites of synaptotagmin I and PLC-δ1 are apparent from these studies: first, only one of the two calcium ions is found at a common position, and second, CBR2 of the SytI C2 domain is not involved in calcium binding.

The present crystallographic study was initiated to characterize the calcium binding sites of PLC-δ1 in more detail. Here we report the structures of the catalytic core of PLC-δ1 in complex with calcium and its analogues barium and lanthanum. The 2.5 Å structures of these complexes enable us to derive the geometry of the metal binding sites in the C2 domain. The observation of a ternary metal binding site in the PLC-δ1/lanthanum complex suggests a general view of how multiple calcium ions may bind to C2 domains.

METHODS

Crystallographic Analysis of PLC-δ1 Complexes. The catalytically active deletion variant Δ(1–132) PLC-δ1 which lacks the N-terminal PH domain was expressed, purified, and crystallized as described (Essen et al., 1996). Crystals were presoaked for at least 6 h in freezing solution (34% w/v PEG 400, 0.4 M sodium acetate, pH 5.65) before being soaked in 1 mM calcium chloride, 1 mM lanthanum (III) chloride, or 20 mM barium acetate for 6, 2, and 11 h, respectively. At concentrations greater than 1 mM the crystals soaked in calcium showed extensive disorder in their diffraction. Data sets from barium and calcium soaks were recorded on a 30 cm MAR imaging plate at Synchrotron Radiation Source (SRS) beamline 9.6, Daresbury, U.K.; lanthanum data were recorded at ESRF beamline BL4/ID2, Grenoble. Data reduction, scaling, and merging were performed with the MOSFLM program package (Leslie, 1992) and the CCP4 suite of programs (CCP4, 1994).

The structures of the complexes were subjected to stereochemically restrained least-squares refinement with TNT-5E (Tronrud et al., 1987) using tight noncrystallographic symmetry restraints throughout the refinement. The protein part of the 2.3 Å structure of a PLC-δ1/Ca^{2+}/1,4,5-IP$_3$ complex (PDB entry 1DJX) served as the starting model for each of the complexes (Essen et al., 1996). This model contains two copies, A and B, for Δ(1–132) PLC-δ1 in its asymmetric unit and lacks structural information for residues A133–A199, A443–A486, A511–A513, B133–B157, B446–B483, and B511–B513. A round of domain-wise

Table 1: X-ray Data Collection and Refinement

parameter	calcium and calcium analogue complexes		
	LaCl$_3$	Ba(OAc)$_2$	CaCl$_2$
data collection and processing			
space group	$F4_132$	$F4_132$	$F4_132$
cell dimension (Å)	$a = 397.92$	$a = 398.25$	$a = 398.03$
resolution (Å)	53−2.6	35−2.5	34−2.5
wavelength (Å)	0.89	0.87	0.87
no. of refl	384052	384574	397693
unique refl	81095	92551	90470
R_{merge} (%)[a]	4.2 (17.0)	6.7 (27.1)	7.3 (29.6)
completeness (%)	98.5 (90.2)	99.7 (99.9)	98.0 (97.1)
redundancy	4.8 (2.9)	4.1 (4.1)	4.0 (4.1)
$\langle I/\sigma(I)\rangle$[b]	28.0 (7.3)	19.7 (4.6)	17.3 (3.8)
refinement			
resolution	10.0−2.6	10.0−2.5	10.0−2.5
R-factor (%)[c]	0.21	0.21	0.21
R_{free} (%)[d]	0.26	0.27	0.28
no. of refl	77696	88488	86499
weighted rmsd from ideality[e]			
bond lengths (Å)	0.015	0.012	0.012
bond angles (deg)	1.42	1.33	1.29
planarity, trigonal (Å)	0.016	0.015	0.014
planarity, others (Å)	0.014	0.013	0.013
torsional angle (deg)	19.2	18.9	18.8
total no. of atoms	9156	8433	9373
no. of water molecules	729	756	909
mean B value (Å^2)[f]	36 (50)	41 (54)	41 (54)

[a] $R_{merge} = (\sum\sum|I_j(h) - \langle I(h)\rangle|/(\sum\sum I_j(h)) \times 100$; values in parentheses correspond to the highest resolution shell. [b] As calculated with the program TRUNCATE (CCP4, 1994). [c] $R = \sum||F_o| - k|F_c||/\sum|F_o|$ with k as the scaling factor. [d] Free R-factor calculated with 4% of the data not used during refinement. [e] With respect to the Engh and Huber parameters (Engh & Huber, 1991). [f] Values in parentheses are for waters.

rigid body refinement followed by positional and B-factor refinement reduced the R-factors (R_{free}) from 33−42% (35−44%) to 26−28% (30−33%) for the three data sets. The introduction of metal atoms and water molecules in SIG-MAA-weighted difference density maps (Read, 1986) followed a strategy previously described for complexes with substrate analogues (Essen et al., 1996, 1997). The flexible portion of CBR1 (residues 643−650) was omitted from refinement and map calculation prior to rebuilding. With the exception of minimal distances between the metal and ligand atoms, i.e., 1.2 Å for metal−oxygen pairs, no other stereochemical restraints were given for the coordination geometry of bound metal atoms. The binding of calcium ions to PLC-δ1 could be only indirectly inferred from electron density maps: the modeling of water molecules instead of calcium at such presumed binding sites led to B-factors for these waters that were significantly lower than that of adjacent protein residues. Occupancies and B-factors for the metal atoms were finally refined in TNT-5E (Tronrud et al., 1987) by restraining the range of B-factors for the metal atoms to the range of B-factors found for their ligands.

Data processing and refinement statistics of the complexes are summarized in Table 1. The barium and calcium complexes show no electron density for residues Lys B648−Asn B649 in CBR1 in addition to the disorder of the parental structure. In the lanthanum complex, the side chains of Lys 643, Lys 646, and Lys 648 are either partially or completely absent in the electron density map.

Because a portion of CBR1 was not well defined in the originally reported structure of the native enzyme (Essen et

al., 1996) (PDB entry 1isd), an effort was made to rebuild the native structure in this region. The water structure was first rebuilt using the protocol described previously (Essen et al., 1997), and an omit map was calculated for a model of the enzyme in which CBR1 was omitted in both molecules. The CBR1 was then rebuilt into the OMIT density and subjected to restrained least-squares refinement with TNT-5E. In the final difference electron density map, no density was visible for residue 649 in either molecule. The final R-factor for the rebuilt model was 22.8 (R_{free} 28.6) for all data between 15.0 and 2.5 Å.

RESULTS AND DISCUSSION

Topological Variants of the C2 Domain. From the structures of the SytI and PLC-δ1 C2 domains it became apparent that there are at least two different topological variants of the C2 domains (Essen et al., 1996) (Figure 2). The PLC-δ1-like variant (P-variant) is circularly permuted relative to the synaptotagmin-like variant (S-variant): the SytI C2 domain starts with a β-strand analogous to β8 in PLC-δ1 and continues with a strand analogous to β1 in PLC-δ1. Consequently, synaptotagmin topology puts N- and C-termini on the same end of the β-sandwich as the CBR's whereas PLC topology has N- and C-termini on the opposite end. Despite these topological differences, the calcium binding region remains unaffected (Figures 2B and 5). Because biochemical characterization of C2 domains has been often carried out with the isolated modules, it is important that the domain boundaries be correctly chosen, since they can affect protein stability or folding. On the basis of alignments of C2 domain sequences (Brose et al., 1995; Ponting & Parker, 1996), we classified the C2 domains from various proteins according to their predicted topologies (Figure 2). The choice of topology was based primarily on the presence (S-variant) or absence (P-variant) of an alternating pattern of hydrophobic and hydrophilic residues aligning with the first strand of SytI C2A. Those domains classified as P-variants have a pattern of hydrophobic residues consistent with a β-strand aligning with β8 of PLC-δ1. Other C2 domains not listed in Figure 2 have a pattern at their termini that makes their relationship to the SytI C2A or the PLC-δ1 C2 domain ambiguous. Although this classification is speculative, we believe it may be a useful guide for the selection of domain boundaries for studies of isolated domains.

In multidomain proteins, it is commonly observed that the relative positions of modules in related sequences vary; for example, in the cPKC's the C1 domains precede the C2 domain while in the nPKC's they follow the C2 domain (Ponting & Parker, 1996). To accommodate the module order swap, but still maintain interdomain packing, the proteins could change the linker lengths between modules. An alternative would be to change the topology by a circular permutation so as to move the N- and C-termini from one end of the domain to the other. In the PKC's the domain order swap is apparently accompanied by both a change in the linker length and a change in the C2 domain topology.

Calcium Binding Region of the PLC-δ1 C2 Domain. The relatively low electron density of calcium makes the identification of calcium ions in electron density maps nontrivial and usually relies on high-resolution data or the recognition of a high coordination number. In order to circumvent this
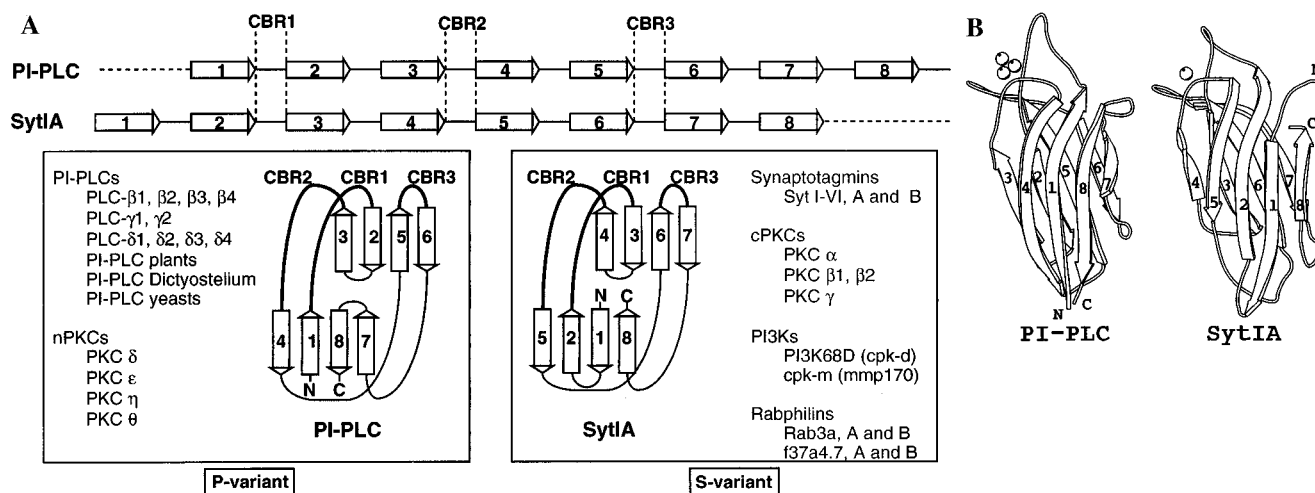
FIGURE 2: Topological variants of the C2 domain. (A) The linear representation of the C2 domains from PLC-δ1 and SytI C2A illustrates that the two domains represent a circular permutation in which the first strand of PLC-δ1 corresponds to the second strand of SytI C2A. The topology of the P-variant (PLC-δ1) and the S-variant (SytIA) C2 domains and the position of the three loops that form the calcium binding region (CBR) are shown below. The C2 domains from various proteins are classified according to their predicted topologies. (B) A schematic drawing of the three-dimensional structures of the PLC-δ1 and SytIA C2 domains.

problem and to allow unambiguous mapping of calcium sites with low affinity and/or high intrinsic mobility, we employed the electron-dense calcium analogues barium and lanthanum. In addition to binding in the C2 domain, these calcium analogues also bind, like calcium, in the active site of the catalytic TIM-barrel domain which was previously described in detail (Essen et al., 1996, 1997).

The calcium binding region of the C2 domain is occupied by at least two metal ions in all complexes studied. The relatively high temperature factors and partial occupancies of the metal ions suggest binding affinities comparable to the millimolar concentrations used under soaking conditions. An analogous behavior is also observed for the catalytic calcium site of the TIM-barrel domain (Table 2). This site adopts full occupancy and lowered B-factors only after binding substrate analogues which apparently stabilize this calcium site by taking part in its coordination (Essen et al., 1997).

Although the metal binding sites can be easily distinguished by their appearance in difference electron density maps (*e.g.*, Figure 3B), the most unambiguous assignment for bound metal ions can be done for the lanthanum ions due to their strong anomalous dispersion. A 3.0 Å anomalous difference Fourier map calculated with solvent-flattened MIR phases clearly reveals the presence of three lanthanum ions in the C2 domain of PLC-δ1 (sites I–III; see Figure 3A). These three ions are bound in a crevice at one end of the C2 domain. The sides of this crevice are formed by the loops CBR1 and CBR3 and closed at one end by CBR2. The geometry of this ternary binding site after refinement is shown in Figure 3C. The separation of 4.1 Å between sites I and II and 3.6 Å between sites II and III is in the range observed for other binary calcium binding sites (Weis et al., 1992; Emsley et al., 1994). Each of the lanthanum ions has a coordination sphere that is derived from octahedral geometry and contains one bidentate aspartate ligand at one of its vertices. The lanthanum in site I adopts a square-pyramidal coordination geometry by liganding two water molecules and the protein ligands Ile 651 and Asp 653 of CBR1 and Asn 677 of CBR2. Asn 677 is the only contribution of CBR2 to metal binding. Ile 651 binds the

Table 2: Metal Coordination in PLC-δ1 Complexes

	distances (Å)[a]					
	LaCl$_3$		BaCl$_2$		CaCl$_2$	
metal ligand	A	B	A	B	A	B
Metal Site I, C2 Domain						
Ser 650 OG	3.0		3.2			
Ile 651 O	2.5	2.3	2.4	2.8	2.1	2.8
Asp 653 OD1	2.6	2.4	3.1	2.8	2.5	3.5
Asp 653 OD2	2.5	2.7	3.1		2.6	2.6
Asn 677	2.3	2.5	2.8	2.9	2.2	2.4
WAT	2.2	2.3		2.7	3.0	2.7
WAT	3.2	2.8			2.7	3.4
occupancy	0.75	1.0	0.4	0.4	0.6	0.8
B-factor (Å^2)	68	83.0	96	95	52	66
Metal Site II, C2 Domain						
Asp 653 OD2	2.5	2.2	3.3		2.8	
Asp 706 OD1	3.4	3.2	3.6	3.3		
Asp 706 OD2	2.8	2.6	3.0	2.8	2.7	2.8
Tyr 707 O	2.4	2.5	2.8	2.8	2.1	2.0
Asp 708 OD1	2.5	2.3		3.1	3.5	2.8
WAT	2.6	2.5			3.6	2.5
WAT	3.6	3.1				
occupancy	0.5	0.6	0.4	0.4	0.6	0.6
B-factor (Å^2)	82	72	97	87	52	54
Metal Site III, C2 Domain						
Asp 706 OD1	3.4	3.0				
Asp 708 OD1	2.9	3.0				
Asp 708 OD2	2.7	2.8				
Asp 714 OD1	3.0	2.6				
WAT	3.5	3.4				
occupancy	0.6	0.5				
B-factor (Å^2)	74	86				
Catalytic Metal Site, TIM Barrel						
Asn 312 OD1	2.6	2.6	2.8	2.65	2.5	2.8
Glu 341 OE1		3.5		3.6	3.0	
Asp 343 OD1	2.7	2.8	2.9	3.0	3.1	2.9
Asp 343 OD2	2.6	2.6	3.1	2.7	3.6	2.4
Glu 390 OE1	2.6	2.8	2.8	2.9	3.5	2.9
WAT	3.6	3.3	3.2	3.5	3.5	
WAT	2.7	2.8	2.7	3.2	2.8	2.4
occupancy	0.75	1.0	1.0	1.0	1.0	1.0
B-factor (Å^2)	70	74	42	43	57	54

[a] For each distance, the values are given for PLC-δ1 monomers A and B.

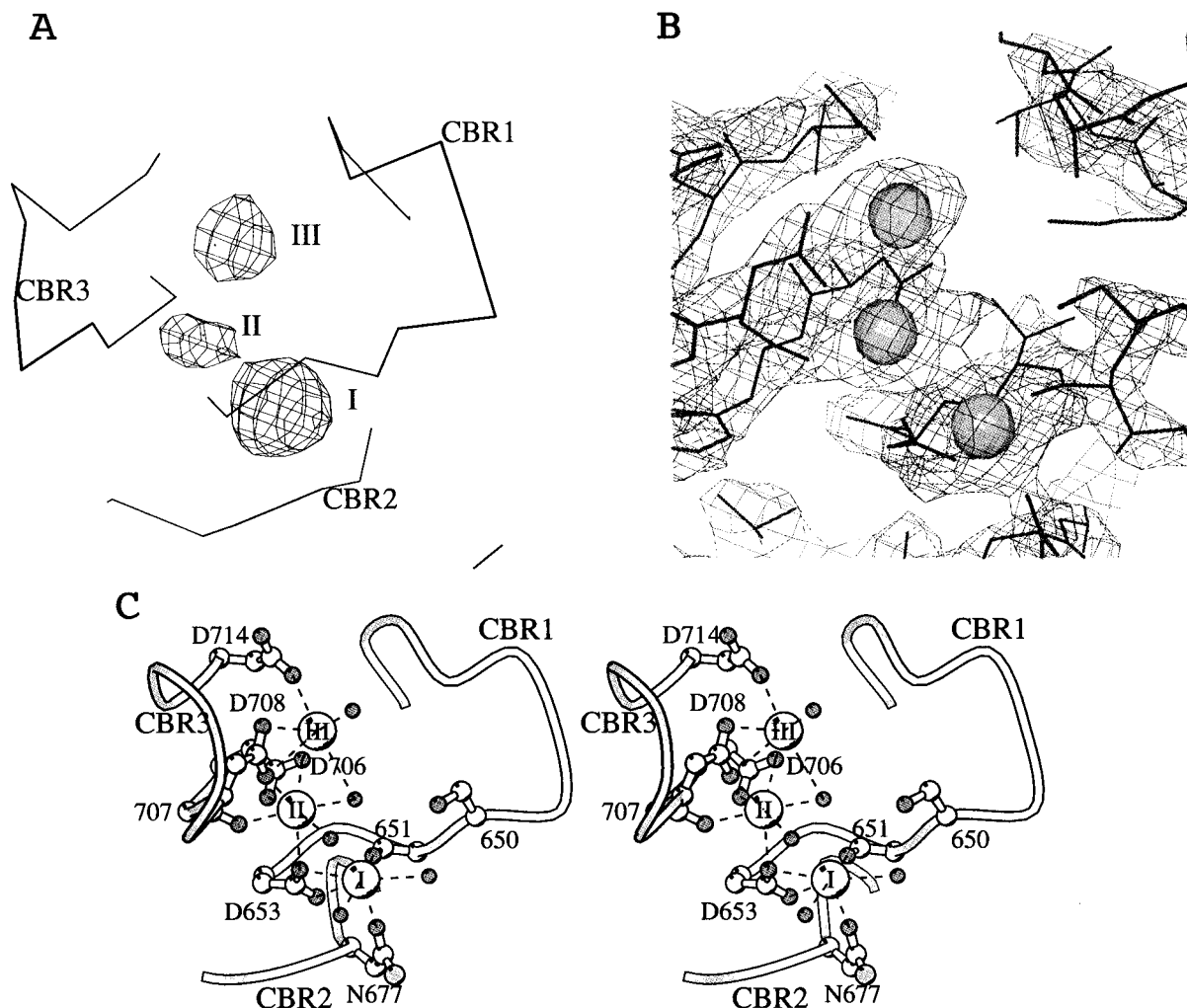lanthanum ion with its carbonyl oxygen whereas the other ligands involve side-chain atoms. A coordination of the

FIGURE 3: Ternary lanthanum binding site in the C2 domain of PLC-δ1 (molecule B). (A) Anomalous difference Fourier of the ternary lanthanum binding site in the PLC-δ1/La^{3+} complex calculated at 3.0 Å resolution and contoured at 3.5σ. The peak heights for sites I, II, and III are 10.5σ, 4.5σ, and 6σ, respectively. (B) A 2.6 Å resolution $m|F_o| - D|F_c|$ map of the refined PLC-δ1/La^{3+} complex contoured at 0.9σ. (C) Stereoview into the metal binding region of the PLC-δ1 C2 domain. Carbon atoms are depicted as white spheres, oxygens and nitrogens as gray shaded spheres, and lanthanum ions as larger spheres. PLC-δ1 is in the same orientation as in the upper panel of Figure 1. All interactions between the lanthanum ions and water and protein ligands listed in Table 2 are shown as dashed lines.

hydroxyl group of Ser 650 to the site I metal ion is found exclusively in molecule A due to slightly different CBR1 conformations between the two PLC-δ1 molecules in the asymmetric unit. Asp 653 is the major ligand in site I by coordinating the metal ion in a bidentate fashion. Site II has an octahedral coordination of metal ion consisting of two water molecules and the protein ligands which reside on CBR1 and CBR3. These ligands are the side chain of Asp 653 (on CBR1) and the side chains of Asp 706 and Asp 708 and the backbone carbonyl oxygen of Tyr 707 (on CBR3). The bidentate ligand of the site II ion is Asp 706, which is centrally located on the floor of the calcium binding region. Site III is exclusively formed by residues on CBR3. This site lacks ordered water ligands, but the orthogonal arrangement of the protein ligands Asp 706, Asp 708, and Asp 714 around the site III lanthanum is consistent with octahedral geometry.

The barium and calcium complexes show binding similar to that of lanthanum, except that site III is apparently not occupied by these metal ions. In the calcium and barium complexes, the side chain of Lys 646 makes salt links with the acidic residues which bind the metal ion at site III in the lanthanum complex. In the lanthanum complex, the side

chain of Lys 646 is disordered. Water ligands can be delineated for site I of the calcium complex which adopts the same square-pyramidal geometry as found in the lanthanum complexes (Figure 4). In site II of molecule B, Asp 708 remains in the coordination sphere for both the barium and the calcium complexes, while in molecule A, this residue undergoes some conformational change by changing its χ_1 angle from a gauche$^-$ to a trans conformer so that its carboxyl group no longer binds the metal.

Experiments on the metal dependence of phospholipid binding and homooligomerization (Davletov & Südhof, 1993, 1994; Sugita et al., 1996) of synaptotagmin C2 domains showed that the function of calcium can be replaced by the calcium analogues barium and strontium, but not by magnesium. Analysis of the cooperativity of calcium binding to a variety of C2 domains suggests that these domains may all have multiple calcium binding sites as evidenced by Hill coefficients for Ca^{2+}-dependent phospholipid binding: between 2.0 and 3.1 for the C2A domain of Syt I (Davletov & Südhof, 1993); three for the C2A domain of Doc2β (Kojima et al., 1996); three for the C2A domain of SytIV (Fukuda et al., 1996). Therefore, we expect that the observation of three lanthanum ions may resemble calcium binding to the PLC-
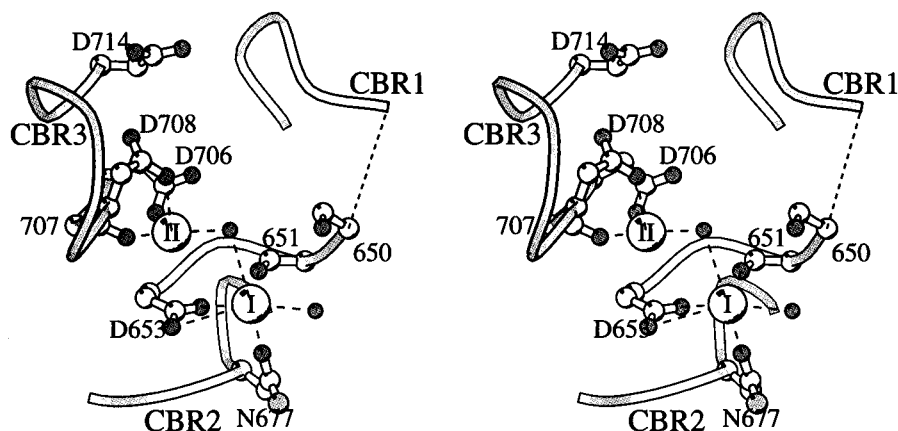
FIGURE 4: Stereo representation showing the binding of calcium in the CBR of the PLC-δ1 C2 domain (molecule B) illustrated as described in Figure 3. The dashed line connects across a region of main-chain disorder (residues 648 and 649).

δ1 C2 domain either with or without suitable phospholipid ligands. An important feature of the PLC-δ1/metal complexes is the presentation of a cluster of waters bound to the metal ions on the surface of the ternary binding site. Ligands such as phospholipids or proteins could bind to the C2 domain by replacing these waters. Such a binding mode would likely lead to highly cooperative calcium binding in the presence of such ligands. The inability of magnesium to functionally substitute for calcium in the C2 domain might be a result of the irregular octahedral coordination geometries in the calcium binding region which can be assumed by calcium and calcium analogues, but not by magnesium (McPhalen et al., 1991).

The model of a ternary calcium binding site reconciles two earlier observations. Sites I and II are the principal metal binding sites that are present in all metal complexes of PLC-δ1, with calcium, barium, lanthanum, and samarium. Sites II and III correspond structurally to the calcium binding site in the synaptotagmin C2A domain that was derived by a combination of molecular dynamics simulations, NMR, and X-ray data (Shao et al., 1996). The failure to observe site III in the complexes of PLC-δ1 with calcium, barium, or samarium was similarly encountered in the X-ray analysis of the synaptotagmin C2 domain, where only the site II calcium ion was crystallographically revealed. Difficulties in the crystallographic assignment of calcium binding sites on the surface of C2 domains might arise from interference by the crystal lattice or from low intrinsic affinities in the absence of suitable ligands such as phospholipids. Because PLC-δ1 crystals are disordered by soaking in calcium solutions more concentrated than 1 mM, it is not known whether site III observed for lanthanum might also be occupied by calcium at higher concentrations or in the presence of phospholipids. A low affinity for calcium of these surface-exposed binding sites was demonstrated for the synaptotagmin C2 domain. In the absence of phospholipids, the microscopic dissociation constants of the SytI C2 domain for calcium were estimated to be 60 μM for site II and 400 μM for site III (Shao et al., 1996) whereas cooperative calcium binding in the presence of acidic phospholipids achieves half-saturation already at concentrations of 3−4 μM (Davletov & Südhof, 1993).

CBR Conformations. The loops CBR1 and CBR3 belong to the most flexible regions of the PLC-δ1 catalytic core with average backbone *B*-factors between 50 and 75 Å^2. Their mobility, as inferred from *B*-factors, remains high even

in the presence of metal. Only in the case of the PLC-δ1/ lanthanum complex is there a decrease, 10−15 Å^2, for the average *B*-factors of these loops in comparison to the native PLC-δ1 structure. Considering their high flexibility, there is no significant conformational change which can be strictly associated with the metal binding (Figure 5A). The conformations of the CBR loops found in the metal complexes are also present in the metal-free, native PLC-δ1 structure. The only major structural change is found in the CBR1 loop. The native enzyme structure showed differences in CBR1 between the two molecules in the asymmetric unit. The conformation of CBR1 for one of the molecules (molecule A) was similar to that seen in the enzyme/metal complexes, whereas the second molecule (molecule B) had a more "closed" conformation for this loop (Figure 5A). The superposition of all the molecules from the native and three metal complex structures, each with two molecules in the asymmetric unit, reveals that only molecule B of the native structure has a CBR1 conformation significantly different from the rest of the molecules. This could be influenced by the crystal contacts this loop is forming with symmetry-related copies of itself around a 3-fold crystallographic axis. In contrast, the CBRs of molecule A are not influenced by such crystal contacts. The lack of major metal-dependent CBR loop movements in the cubic crystals of PLC-δ1 differs from the changes described in a 3.0 Å structure of PLC-δ1 in a triclinic unit cell upon binding the lanthanide samarium (Grobler et al., 1996). Binding of samarium in the triclinic crystals was accompanied by a conformational change in the CBR, mainly CBR1, from a "closed" to an "open" state. The structures described here show that even the metal-free PLC-δ1 can acquire an open conformation in CBR1. The open conformation might be further stabilized by metal binding as suggested by the observation that all metal complexes have the open conformation and that the closed conformation is observed only in the absence of metal.

The conformation of the CBR3 loop is not only unchanged among the structures of PLC-δ1 but is also very similar to the conformation of CBR3 in the SytI C2A domain (Shao et al., 1996). A superposition of the backbone atoms of CBR3 in PLC-δ1 and SytI gives an rmsd of 1.2 Å and shows an identical orientation of all peptide groups in the loop (Figure 5B). In PLC-δ1, the base of this "canonical" CBR3 loop is stabilized by hydrogen bonds between its own calcium ligands and the calcium ligand Asp 653 of CBR1 (Asp 706 OD2−Asp 653 N, 2.9 Å; Tyr 707 N−Asp 653 O,
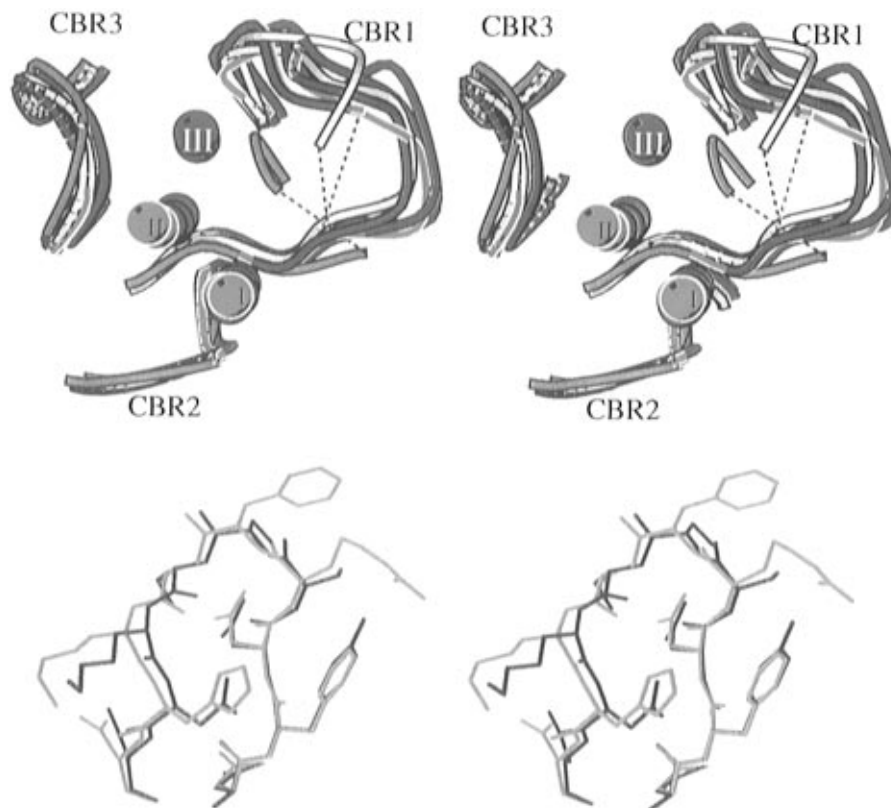
FIGURE 5: Stereo diagram showing a superposition of the structures of the calcium binding regions in the C2 domains from PLC-δ1 and synaptotagmin I. (A, top) Overall view showing bound metal ions and the C_α traces of CBR1, CBR2, and CBR3. The native PLC-δ1 structure is shown in white, the PLC-δ1/La^{3+} complex in blue, the PLC-δ1/Ca^{2+} complex in green, the PLC-δ1/Ba^{2+} complex in red, and the SytI C2 domain in orange. Loops for both molecules A and B of PLC-δ1 are shown. Dashed lines connect across regions of main-chain disorder in the crystal structures. (B, bottom) Structural comparison between the CBR3 loops of the PLC-δ1 (black) and the SytI C2A (orange) domains.

2.8 Å). The tip of the CBR3 loop is apparently cross-linked by a water molecule that forms hydrogen bonds with the carbonyl oxygens of Asp 708 and Asp 711 (2.4, 2.4 Å) and the amide side chain of Asn 713 (2.6 Å). These stabilizing interactions, in particular the bridging water molecule, can also be found in the SytI C2A domain.

Modeling Calcium Binding Regions in Other C2 Domains. One intriguing question is how typical the ternary metal binding site of the PLC-δ1 C2 domain is for other C2 domains. In the SytI C2 domain, five aspartate residues were proposed to represent a signature sequence called the C2 motif that is conserved in the calcium binding region of many C2 domains (Shao et al., 1996). These residues were used to construct a model for a binary calcium binding site in the SytI C2A domain, and a unifying nomenclature for the calcium binding residues in CBR1 and CBR3 was proposed: residues in CBR1 were labeled with the symbol X (X1 and X7 in SytI C2A), and those in CBR3 were labeled with the symbol Y (Y1, Y3, and Y9 in SytI C2A) (Shao et al., 1996). Four of five residues of the C2 motif are also present in the PLC-δ1 C2 domain (Asp 653, Asp 706, Asp 708, and Asp 714, equivalent to residues X7, Y1, Y3, and Y9 of SytI C2A). The synaptotagmin-based model of a binary calcium site differs from our structure of a ternary site by the absence of the site I calcium ion. In addition, the binary model of SytI C2A calcium binding involves Asp 172 (residue X1) whereas its equivalent in PLC-δ1 (Asn 645) is not a metal ligand. The participation of Asp 172 in binding the site II calcium ion was not observed in the crystal structure of the SytI C2A domain where this residue and

the subsequent residues (173−175) of CBR1 were disordered (Sutton et al., 1995). However, in a superposition of C2 domains from synaptotagmin I and the PLC-δ1/lanthanum complex, a residue at the X1 position is equally close to site I and II lanthanum ions. A ternary calcium binding site in the SytI C2A domain may be possible, with Asp 172 and Asp 178 as the primary ligands for a site I calcium (such as modeled in Figure 6A,C). Additional ligands for a site I calcium in the SytI C2A domain might be derived from residues in CBR1 and CBR2. CBR2 would not be involved in ligation in the same way as in PLC-δ1 because it has a lysine residue at the position corresponding to the PLC-δ1 CBR2 metal ligand, Asn 677. The reported NMR data (Shao et al., 1996) might also be interpreted in terms of a ternary calcium binding region in the SytI C2A domain (because SytI D172 and D178 could be ligands for both sites I and II, the Ca^{2+}-induced changes in the chemial shifts would be similar for these two sites). Although the results of Shao et al. have been interpreted in terms of a binary calcium binding site (sites II and III), a ternary binding site would be consistent with observations of Hill coefficients of about 3 obtained for calcium-dependent phospholipid binding studies of the SytI C2A domain (Davletov & Südhof, 1993). The assumption of a site I calcium in synaptotagmin would explain the significant changes in the backbone resonances observed for CBR2, because site I is adjacent to CBR2.

It is likely that other C2 domains containing the C2 motif bind an array of calcium ions like PLC-δ1 and presumably synaptotagmin I (Figure 6). Site I would be predominantly associated with CBR1, site III with CBR3, and site II would
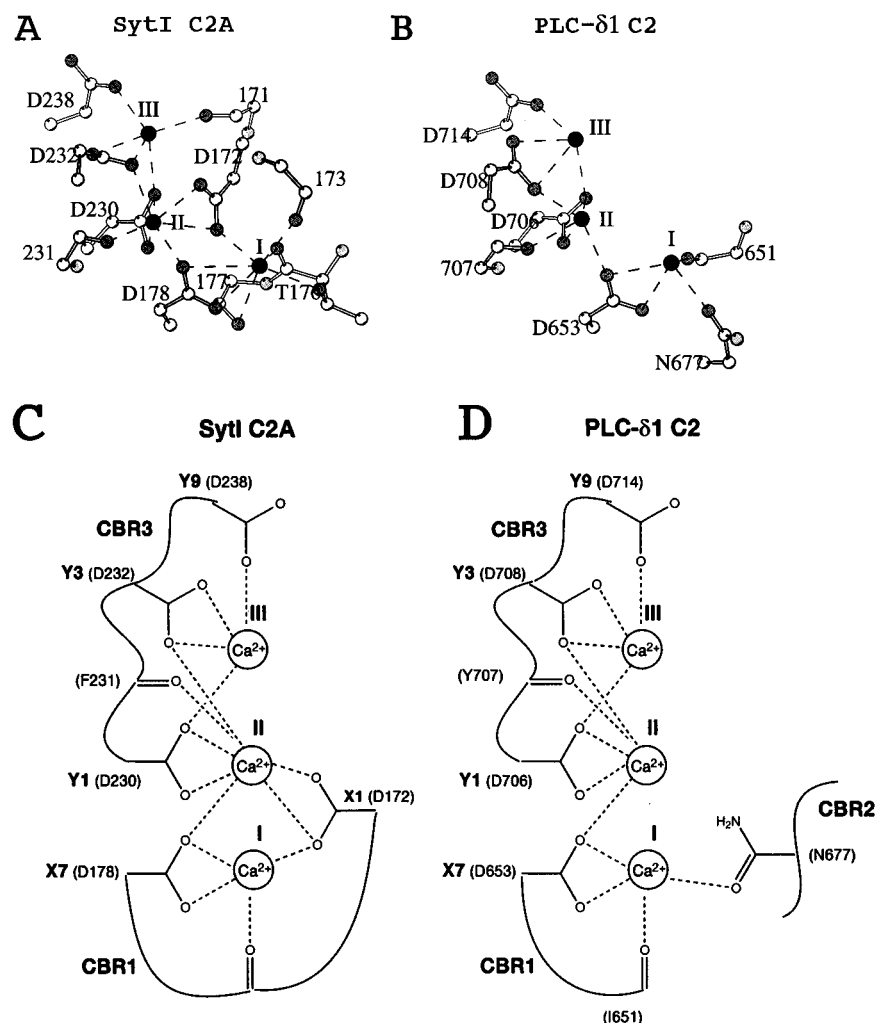
FIGURE 6: Structural model of a ternary calcium binding site in the SytI C2A domain. (A) Ball-and-stick representation of a putative model of a ternary calcium binding site in the SytI C2A domain, based on the structure of the SytI C2A and the ternary calcium binding as observed in PLC-δ1. (B) Ternary calcium binding site in the PLC-δ1 C2 domain. Carbon atoms are depicted as white spheres, oxygens and nitrogens as gray shaded spheres, and metal ions as black spheres. Interactions between the metal ions and protein ligands are shown as dashed lines. (C, D) Schematic comparison of the proposed ternary calcium binding site in the C2 domain of (C) SytIA and (D) PLC-δ1. The proposed SytIA ternary calcium binding incorporates site II identified in the X-ray structure, site III described from a combination of NMR spectroscopy and molecular dynamics simulations, and site I based on analogy with the PLC-δ1 metal binding site. In addition to D172 and D178 ligands, site I could have carbonyl oxygens from other residues in CBR1 and CBR2 as ligands.

be shared between these two loops. In some cases like the cPLA$_2$ C2 domain, a ligand derived from CBR2 might be involved in binding the site I calcium similarly as in PLC-δ1 [see the alignment in Brose et al. (1995)]. This novel type of a calcium binding site might explain the high cooperativity of calcium-mediated lipid binding by C2 domains.

Role of C2 Domains in PI-PLCs. Although the membrane-binding capability and functional role are still unknown for the PLC-δ1 C2 domain, the presence of a conserved C2 motif in the calcium binding region suggests that the C2 domain of PLC-δ1 could be involved in calcium-dependent phospholipid binding similarly to the SytI C2A domain. Mutational studies showed that the presence of the C2 domain, but not of the membrane-anchoring PH domain, is essential for catalytic activity of PLC-δ1 (Cifuentes et al., 1993; Ellis et al., 1993). We suggested on the basis of the coplanar nature of the active site and the calcium binding region of the C2 domain that the C2 domain might assist in proper positioning of the catalytic TIM-barrel domain onto the membrane (Essen et al., 1996). The binding energy of the

catalytic core to lipid membranes should be small, less than 2 kcal/mol, because intact PLC-δ1 and the isolated PLC-δ1 PH domain bind with comparable affinities to lipid vesicles of specific composition (Garcia et al., 1995). However, the binding energy derived from the interaction of the C2 domain with the membrane could compensate for an energetically unfavorable membrane penetration by parts of the catalytic domain. Studies on the dependence of enzyme activity and membrane surface pressure gave a lower limit of 1 nm^2 for the protein surface area penetrating the membrane (Rebecchi et al., 1992a). A candidate for such a surface region is a hydrophobic ridge that surrounds those parts of the active site which are close to the C2 domain (Essen et al., 1996).

Among PI-PLC's the CBR regions of C2 domains vary in number of putative calcium ligands and length of the loops. Plant PI-PLC's appear to have a set of calcium ligands in their CBRs analogous to SytI C2A or PLC-δ1. Plant PI-PLC's are membrane associated yet do not have the PH domain that serves as the principal membrane tether in PLC-δ1 (Hirayama et al., 1995; Shi et al., 1995). The C2 domains may assume the role of a membrane tether for this class of
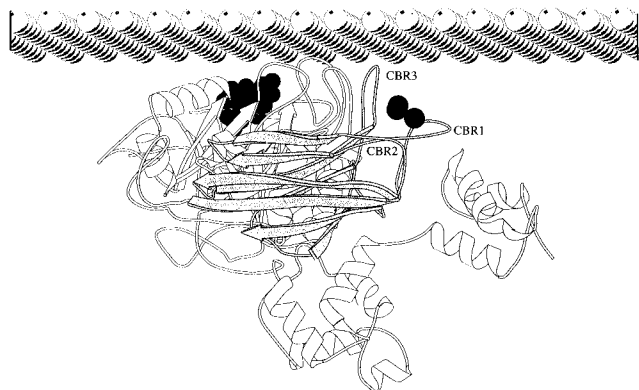
FIGURE 7: Docked model of the catalytic core of PLC-δ1 on a lipid membrane represented by a layer of spheres. The 1,4,5-IP$_3$/Ca^{2+} complex in the active site of the catalytic domain is shown in CPK representation, and the lanthanum sites in the C2 domain are shown as spheres. Strand β3 (analogous to strand 4 from SytI C2A) that would run closest to and roughly parallel to the interface is labeled.

enzymes. PLC-β's (β1−β4) contain only truncated CBR1 loops and short β-hairpins for CBR3 which appear to lack most of the potential calcium ligands. The γ-isozymes (γ$_1$,γ$_2$) are between these two extremes. Like PLC-β's, they lack ligands in CBR1 loops but resemble PLC-δ's by having putative calcium ligands in CBR2 and CBR3. The membrane binding function for isozymes lacking most of the CBR calcium ligands in their C2 domain may be augmented by protein−protein interactions, *e.g.,* with membrane-anchored G-proteins in the case of PLC-βs. Alternatively, membrane binding in PI-PLCs other than the δ-isozymes might be assisted by the presence of additional basic residues in their strand β3 that could interact with anionic phospholipid head groups (Figure 7).

Membrane Binding by C2 Domains. The calcium-mediated interaction of C2 domains with lipid membranes might be accomplished in two different ways: in a bridging mechanism, calcium ions might be directly involved in membrane binding by being sandwiched between the protein and the phosphoryl groups of phospholipids. Such a bridging role of calcium has been suggested for annexins, various pentraxins, and the membrane-anchoring GLA domains of some blood coagulation factors and structurally demonstrated for annexin V (Swairjo et al., 1995). In an alternate mechanism, the binding of calcium ions to the C2 domain would only indirectly affect the affinity of C2 domains for lipid membranes by changing the domain structure or electrostatic characteristics (Newton, 1995). The calcium-induced structural transitions of GLA domains to membrane binding competent forms exemplify this mechanism (Sunnerhagen et al., 1995).

The structures of PLC-δ1 complexed with calcium or calcium analogues do not support the involvement of major structural changes triggered by metal binding. The open, crevice-like nature of the calcium binding region would allow access for the head groups of up to two phospholipid molecules. Each of these phospholipids would be able to interact directly with the bound calcium ions *via* its phosphoryl group. Basic residues nearby, Lys 646 and Lys 648 on CBR1 and Lys 712 on CBR3, may assist the binding of negatively charged phospholipids in the calcium binding region. Taken together with additional geometric considerations like the observed orientation of the PIP$_2$ head group

in the catalytic TIM barrel (Essen et al., 1996) and the rigid nature of the TIM-barrel/C2-domain interface (Grobler et al., 1996), this bridging mechanism predicts how PLC-δ1 could dock onto a phospholipid membrane (Figure 7). An apparent problem is posed by CBR3, which would have to penetrate partially the lipid membrane or change its conformation to avoid penetration. No significant calcium-induced conformational change of CBR3 was observed for PLC-δ1 or SytI C2 domains. In the SytI C2 domain, the tip of the CBR3 loop is occupied by Phe 234 which might interact with the hydrophobic portion of the membrane. In the PLC-δ1 C2 domain, this position is occupied by a serine residue.

A looser mode of PLC-δ1 binding to membranes would be possible if the calcium binding region only indirectly affected membrane interaction and binding of the catalytic core of PLC-δ1 to the lipid membrane were mainly driven by electrostatic interaction. Calculations with GRASP (Nicholls, 1992) on the surface potential of the PLC-δ1 C2 domain show a dominance of the calcium binding region on the surface charge. In the absence of calcium ions, the C2 domain has largely negatively charged surface characteristics which can be reverted by including calcium ions in the calculation. According to our docking model, β-strand β3 of the PLC-δ1 C2 domain runs almost parallel to the membrane and might employ Arg 665 and Arg 670 for interaction with phospholipid head groups. Interestingly, it is this strand of the C2 domains in other proteins that is rich in basic residues (Newton, 1995) and functions in some C2 domains to bind the highly negatively charged IP$_4$ (Fukuda et al., 1994, 1995; Cullen et al., 1995; Irvine & Cullen, 1996). Other basic regions on the membrane-facing part of the PLC-δ1 C2 domain that might affect interaction with the phospholipid membrane are formed by Lys 646, Lys 648, Lys 655, Lys 712, and Lys 738.

Conclusion. The structure of a ternary metal binding site in the C2 domain of PLC-δ1 gives a unifying concept of how C2 domains bind calcium ions with high cooperativity in the presence of phospholipids. Despite topological differences, the calcium binding regions of the C2 domains from PLC-δ1 and synaptotagmin I differ only in minor details regarding the identity of ligands for site I calcium. Future studies will have to show how calcium affects membrane binding—*via* a bridging mechanism or indirectly—and which additional regions of the C2 domain participate therein.

REFERENCES

Berridge, M. J. (1993) *Nature 361*, 315−325.

Brose, N., Hofmann, K., Hata, Y., & Südhof, T. C. (1995) *J. Biol. Chem. 270*, 25273−25280.

CCP4 (1994) *Acta Crystallogr. D50*, 760−763.

Cifuentes, M. E., Honkanen, L., & Rebecchi, M. J. (1993) *J. Biol. Chem. 268*, 11586−11593.

Cullen, P. J., Hsuan, J. J., Truong, O., Letcher, A. J., Jackson, T. R., Dawson, A. P., & Irvine, R. F. (1995) *Nature 376*, 527−530.

Davletov, B. A., & Südhof, T. C. (1993) *J. Biol. Chem. 268*, 26386−26390.

Davletov, B. A., & Südhof, T. C. (1994) *J. Biol. Chem. 269*, 28547−28550.

Ellis, M. V., Carne, A., & Katan, M. (1993) *Eur. J. Biochem. 213*, 339−347.

Emsley, J., White, H. E., O'Hara, B. P., Oliva, G., Srinivasan, N., Tickle, I. J., Blundell, T. L., Pepys, M. B., & Wood, S. P. (1994) *Nature 367*, 338−345.

Engh, R. A., & Huber, R. (1991) *Acta Crystallogr. A47*, 392−400.

Essen, L.-O., Perisic, O., Cheung, R., Katan, M., & Williams, R. L. (1996) *Nature 380*, 595−602.

Essen, L.-O., Perisic, O., Katan, M., Wu, Y., Roberts, M. F., & Williams, R. L. (1997) *Biochemistry* (in press).

Ferguson, K. M., Lemmon, M. A., Schlessinger, J., & Sigler, P. B. (1995a) *Cell 83*, 1037−1046.

Fukuda, M., Aruga, J., Niinobe, M., Aimoto, S., & Mikoshiba, K. (1994) *J. Biol. Chem. 269*, 29206−29211.

Fukuda, M., Kojima, T., Aruga, J., Niinobe, M., & Mikoshiba, K. (1995) *J. Biol. Chem. 270*, 26523−26527.

Fukuda, M., Kojima, T., & Mikoshiba, K. (1996) *J. Biol. Chem. 271*, 8430−8434.

Garcia, P., Gupta, R., Shah, S., Morris, A. J., Rudge, S. A., Scarlata, S., Petrova, V., McLaughlin, S., & Rebecchi, M. J. (1995) *Biochemistry 34*, 16228−16234.

Grobler, J. A., Essen, L.-O., Williams, R. L., & Hurley, J. H. (1996) *Nat. Struct. Biol. 3*, 788−795.

Hirayama, T., Ohto, C., Mizoguchi, T., & Shinozaki, K. (1995) *Proc. Natl. Acad. Sci. U.S.A. 92*, 3903−3907.

Irvine, R., & Cullen, P. (1996) *Curr. Biol. 6*, 537−540.

Kojima, T., Fukuda, M., Aruga, J., & Mikoshiba, K. (1996) *J. Biochem. 120*, 671−676.

Kraulis, P. J. (1991) *J. Appl. Crystallogr. 24*, 946−950.

Lee, S. B., & Rhee, S. G. (1995) *Curr. Opin. Cell Biol. 7*, 183−189.

Leslie, A. G. W. (1992) *Joint CCP4 and ESF-EACMB Newsletter on Protein Crystallography*, Daresbury Laboratory, Warrington, U.K.

Li, C., Ullrich, B., Zhang, J. Z., Anderson, R. G. W., Brose, N., & Südhof, T. C. (1995) *Nature 375*, 594−599.

McPhalen, C. A., Strynadka, N. C. J., & James, M. N. G. (1991) *Adv. Protein Chem. 42*, 77−143.

Nakashima, S., Banno, Y., Watanabe, T., Nakamura, Y., Mizutani, T., Sakai, H., Zhao, Y., Sugimoto, Y., & Nozawa, Y. (1995) *Biochem. Biophys. Res. Commun. 211*, 364−369.

Nalefski, E. A., Sultzman, L. A., Martin, D. M., Kriz, R. W., Towler, P. S., Knopf, J. L., & Clark, J. D. (1994) *J. Biol. Chem. 269*, 18239−18249.

Newton, A. C. (1995) *Curr. Biol. 5*, 973−976.

Nicholls, A. (1992) *GRASP: Graphical representation and analysis of surface properties*, Columbia University, New York.

Paterson, H. F., Savopoulos, J. W., Perisic, O., Cheung, R., Ellis, M. V., Williams, R. L., & Katan, M. (1995) *Biochem. J. 312*, 661−666.

Ponting, C. P., & Parker, P. J. (1996) *Protein Sci. 5*, 162−166.

Read, R. J. (1986) *Acta Crystallogr. A42*, 140−149.

Rebecchi, M., Boguslavsky, V., Boguslavsky, L., & McLaughlin, S. (1992) *Biochemistry 31*, 12748−12753.

Rhee, S. G., & Choi, K. D. (1992) *J. Biol. Chem. 267*, 12393−12396.

Shao, X., Davletov, B. A., Sutton, R. B., Südhof, T. C., & Rizo, J. (1996) *Science 273*, 248−251.

Shi, J., Gonzales, R. A., & Bhattacharyya, M. K. (1995) *Plant J. 8*, 381−390.

Sugita, S., Hata, Y., & Südhof, T. C. (1996) *J. Biol. Chem. 271*, 1262−1265.

Sunnerhagen, M., Forsén, S., Hoffrén, A.-M., Drakenberg, T., Teleman, O., & Stenflo, J. (1995) *Nat. Struct. Biol. 2*, 504−509.

Sutton, R. B., Davletov, B. A., Berghuis, A. M., Südhof, T. C., & Sprang, S. R. (1995) *Cell 80*, 929−938.

Swairjo, M. A., Concha, N. O., Kaetzel, M. A., Dedman, J. R., & Seaton, B. A. (1995) *Nat. Struct. Biol. 2*, 968−974.

Tronrud, D. E., Ten Eyck, L. F., & Matthews, B. W. (1987) *Acta Crystallogr. A43*, 489−501.

Weis, W. I., Drickamer, K., & Hendrickson, W. A. (1992) *Nature 360*, 127−134.

Yamaguchi, T., Shirataki, H., Kishida, S., Miyazaki, M., Nishikawa, J., Wada, K., Numata, S.-I., Kaibuchi, K., & Takai, Y. (1993) *J. Biol. Chem. 268*, 27164−27170.

Zhang, J. Z., Davletov, B. A., Südhof, T. C., & Anderson, R. G. W. (1994) *Cell 78*, 751−760.